ELSEVIER

Polymer 42 (2001) 1449–1459

polymer

www.elsevier.nl/locate/polymer

Phase separation in miscible polymer blends as detected by modulated temperature differential scanning calorimetry

G. Dreezen[a], G. Groeninckx[a], S. Swier[b], B. Van Mele[b,*]

[a]*Catholic University of Leuven (KU Leuven), Department of Chemistry, Laboratory of Macromolecular Structural Chemistry, Celestijnenlaan 200F, B-3001 Heverlee, Belgium*

[b]*Free University of Brussels (VUB), Department of Physical Chemistry and Polymer Science, Pleinlaan 2, B-1050 Brussels, Belgium*

Received 28 March 2000; accepted 12 June 2000

Abstract

Phase separation of two partially miscible polymer blends is studied with modulated temperature DSC (MTDSC). The lower critical solution temperature (LCST) demixing behavior of poly(ethylene oxide) (PEO) blended with poly(ether sulphone) (PES) and with poly(3,4′-diphenylene ether isophtaloyl amide), as determined by cloud point temperatures with optical microscopy, is in excellent agreement with results obtained from non-isothermal MTDSC measurements. The non-isothermal MTDSC apparent heat capacity evolution is time-dependent. It is influenced by the endothermic demixing enthalpy and, in the case of PEO/PES blends, by the vitrification of a high-T_g phase formed. Quasi-isothermal MTDSC measurements contain information on the kinetics of demixing and remixing, emphasizing the added value of MTDSC to follow in situ the diffusion-controlled phase separation processes of partially miscible polymer blends.

Keywords: Modulated temperature differential scanning calorimetry; Apparent heat capacity; Partially miscible polymer blend

1. Introduction

Partially miscible polymer blends are characterized by a temperature and composition dependent miscibility. Liquid–liquid phase separation of a miscible blend system can occur either during heating (LCST-type) or during cooling (UCST-type). Cloud point temperatures are usually detected by observation of the transmitted light intensity during a temperature change of the blends [1]. The determination of phase separation in partially miscible polymer blends by means of thermal analysis is often difficult because of the small demixing enthalpy and the slow rate of the diffusion-controlled process. It has been shown that differential scanning calorimetry (DSC) can be used to determine miscibility gaps in both low and high molecular weight systems [2]. However, the use of high DSC scanning rates to enlarge the evolved heat flow signal results in poorly resolved signals that are difficult to interpret [3–5]. A different approach in the characterization of phase separation in polymer blends by DSC is based on the detection of the glass transition temperatures of the phase-separated blend by means of enthalpy relaxation effects [6,7].

Modulated temperature differential scanning calorimetry (MTDSC) is an extension of conventional DSC that combines high resolution with high sensitivity by use of a sinusoidal temperature modulation superimposed on a constant temperature or a linear temperature program with a small underlying (average) heating rate [8–10]. These characteristics appear to be suitable for the determination of liquid–liquid phase separation in polymer blends. In comparison to conventional DSC, the MTDSC analysis enables the simultaneous calculation of an additional quantity, the cyclic or (modulus of) complex (specific) heat capacity (in short termed heat capacity), C_p (J g^{-1} K^{-1}):

$$C_p = \frac{A_{HF}}{A_T \omega} \tag{1}$$

where A_{HF} is the amplitude of the cyclic heat flow (W g^{-1}) and $A_T\omega$ is the amplitude of the cyclic heating rate, with A_T the temperature modulation amplitude (K), ω the modulation angular frequency ($= 2\pi/p$) and p the modulation period (s).

A complete description of the extraction of the heat capacity and other MTDSC signals (total heat flow, reversing

* Corresponding author. Fax: +32-2-629-32-78; Tel.: +32-2-629-32-76/88.

E-mail address: bvmele@vub.ac.be (B. Van Mele).

0032-3861/01/$ - see front matter
PII: S0032-3861(00)00532-2

heat flow, non-reversing heat flow, heat flow phase and phase correction) can be found in the literature [8,11,12].

The benefits of the heat capacity information, especially in isothermal conditions, for the characterization of reacting polymers have been illustrated [13–15]. Recently, MTDSC results on the in situ detection of reaction-induced phase separation in thermosetting systems have been reported [16,17].

In this paper, the applicability of MTDSC to study liquid–liquid phase separation in polymer blends will be investigated. The binary blends of poly(ethylene oxide) (PEO), a crystallizable component, with a high-T_g amorphous component, poly(ether sulphone) (PES) or poly(3,4′-diphenylene ether isophtaloyl amide) (Aramide 34I) are chosen as partially miscible polymer systems with LCST-type demixing behavior. These results should contribute to a better understanding of the kinetics of phase separation processes in general, and, more specifically, of phase separation during cure of thermosetting systems [16–19] and during in-situ polymerization [18,20].

2. Experimental

2.1. Blend preparation

2.1.1. PEO/PES

PEO, from UCB, with a viscosity average molecular weight of 17 000 g mol^{-1} and a polydispersity of 1.35, was blended with PES (trade name Victrex 4800G), from Victrex Ltd. (UK), with a viscosity average molecular weight of 61 000 g mol^{-1} and a polydispersity of 1.72. PEO/PES blends of 90/10, 80/20, 75/25, 60/40, 50/50 and 20/80 w/w compositions were obtained by preparing 10% (w/v) solutions of both components in dimethylformamide and by removal of the solvent under vacuum at 70°C. The blends were additionally dried under vacuum at 60°C for 2 days.

2.1.2. PEO/Aramide

PEO with a viscosity average molecular weight of 20 000 g mol^{-1} and a polydispersity of 1.2, from FLUKA Chemie AG, was blended with a laboratory-synthesized Aramide 34I [21] with a weight average molecular weight of 36 000 g mol^{-1} and a polydispersity of 2.04 in w/w compositions of 95/5, 90/10, 80/20, 75/25, 65/35, 50/50 and 20/80. Blends were prepared by solution casting from 10% (w/v) solutions in pyridine. After evaporation of the solvent, the blends were dried under vacuum at 80°C for 2 days to remove the residual solvent.

The glass transition temperatures of PEO and of the amorphous components PES and Aramide 34I are ca. −60°C and 225°C, respectively.

2.2. Optical microscopy

Cloud points were detected from the light transmitted by thin samples between glass slides under an Olympus optical microscope coupled with a computer-controlled CCD-camera. The samples were heated at a rate of 1°C min^{-1} using a Mettler FP-82 hot stage. The onset of the decrease of the transmitted light intensity was chosen as the cloud point temperature.

2.3. Dynamic mechanical thermal analysis

Dynamic mechanical thermal analysis measurements were performed with a DMTA MK-II of Polymer Laboratories. The scans were performed in the bending mode from −70 to 220°C at a heating rate of 2°C min^{-1} and at frequencies of 1 and 10 Hz.

2.4. Fourier-transform infrared spectroscopy

A Perkin–Elmer System 2000 Fourier-transform infrared (FTIR) spectrometer was used for the FTIR experiments. Thin films required for FTIR spectroscopy were prepared from 2% (w/v) solutions on a KBr window. The spectrum was obtained by Fourier transforming 12 accumulated interferograms between 4500 and 450 cm^{-1} at a resolution of 4 cm^{-1}. The samples were heated at 1.5°C min^{-1} in a Mettler FP-82 hot stage.

2.5. Conventional DSC

A Perkin–Elmer DSC-7 with CCA-7 cooling system was used at a heating rate of 10°C min^{-1} under N_2-atmosphere. The sample weight was between 5 and 10 mg. The DSC temperature and enthalpy calibrations were performed using indium and gallium. The Perkin–Elmer system was equipped with a controlled nitrogen atmosphere cover to handle samples at low temperature without condensation prior to the measurement.

2.6. MTDSC

The MTDSC measurements were performed on a TA Instruments 2920 DSC with MDSC™ option and a RCS cooling system. Helium was used as a purge gas (25 ml min^{-1}). Indium and gallium were used for temperature calibration. The former was also used for enthalpy calibration. Heat capacity calibration was performed with a PMMA standard (supplied by Acros [22]), using the heat capacity difference between two temperatures, one above and one below the glass transition temperature of PMMA, to make sure that heat capacity changes were adequately measured. Standard modulation conditions used in the experiments are an amplitude A_T of 1°C and a period p of 60 s. For non-isothermal experiments a heating rate β of 1°C min^{-1} was used.

The samples were molten and thin films were hot pressed in non-hermetic aluminum crucibles, making sure not to surpass the temperature where phase separation occurs. Sample weights were between 5 and 10 mg.

Table 1
Cloud point temperature of PEO/Aramide and PEO/PES blends detected by optical microscopy (1°C min^{-1}), conventional DSC (10°C min^{-1}) and MTDSC ($\beta = 1$°C min^{-1}, $A_T = 1$°C and $p = 60$ s)

Blend composition	Optical microscopy (°C)	Conventional DSC (°C)	MTDSC (°C)
PEO/Aramide			
95/5	133	–	–
90/10	122	121	–
80/20	129	129	131
75/25	135	132	137
65/35	138	140	142
50/50	152	152	150
20/80	186	182	181
PEO/PES			
90/10	74	–	–
80/20	80	80	80
75/25	84	82	82
60/40	97	93	97
50/50	104	103	101
20/80	133	127	130

3. Results and discussion

3.1. Determination of the onset of phase separation

The liquid–liquid phase separation process of PEO/PES and PEO/Aramide blends was first investigated by means of optical microscopy and conventional DSC in order to obtain sufficient information for the interpretation of the MTDSC signals.

3.1.1. Optical microscopy

The cloud point temperatures of PEO/PES and PEO/Aramide blends, as detected by optical microscopy during heating at 1°C min^{-1}, are presented in Table 1. The phase diagrams of both blend systems are given in Fig. 1, showing the experimental cloud point curve in relation to: (i) the melting and crystallization domain; and (ii) the theoretical evolution of the glass transition temperature, T_g, with the composition of the miscible systems. Note that the theoretical evolution of T_g is only indicative and should be corrected by measuring T_g for different one-phase compositions. Also the width of the glass transition region should be considered in this respect.

PEO/Aramide blends exhibit liquid–liquid phase separation of the LCST-type from 125°C at a 90/10 blend composition. PEO/PES blends also show LCST-type phase separation behavior with a minimum temperature of 75°C at a 90/10 blend composition in agreement with literature [23,24].

3.1.2. Conventional DSC

DSC thermograms of the 50/50 blend of both PEO/Aramide and PEO/PES are presented in Fig. 2. To allow the measurement of T_g of the amorphous one-phase blend, the samples were first quenched from a temperature between the melting temperature of PEO and the cloud point

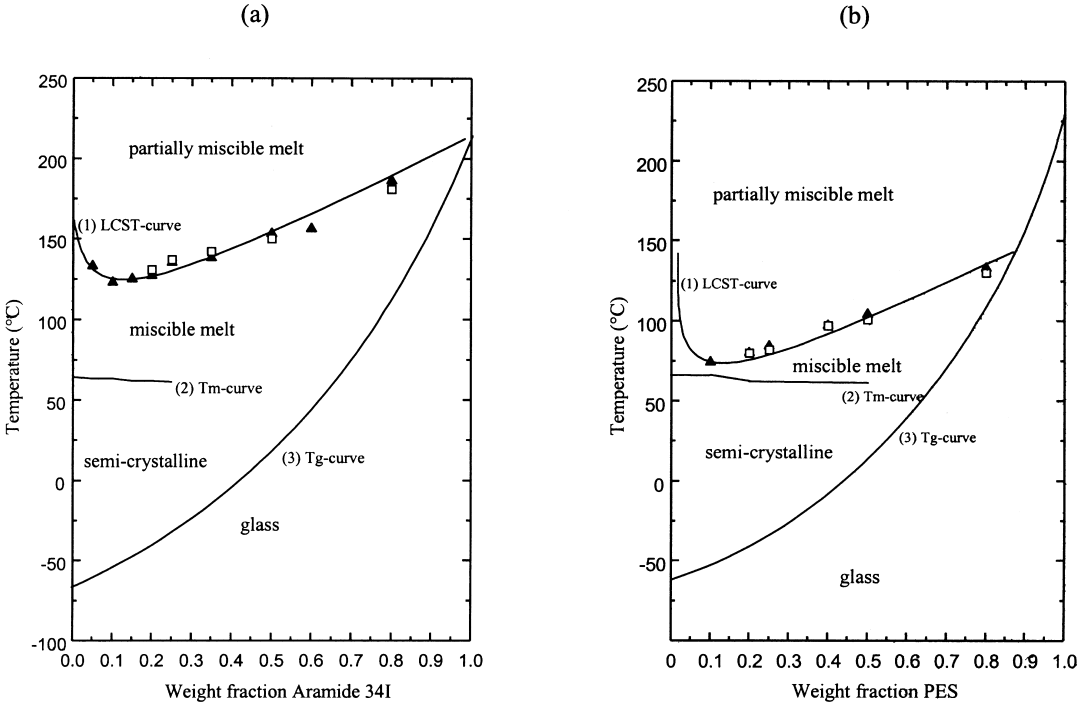

Fig. 1. Phase diagram of: (a) PEO/Aramide; and (b) PEO/PES blend system (▲) cloud point determined by optical microscopy, (□) onset of demixing obtained by MTDSC.

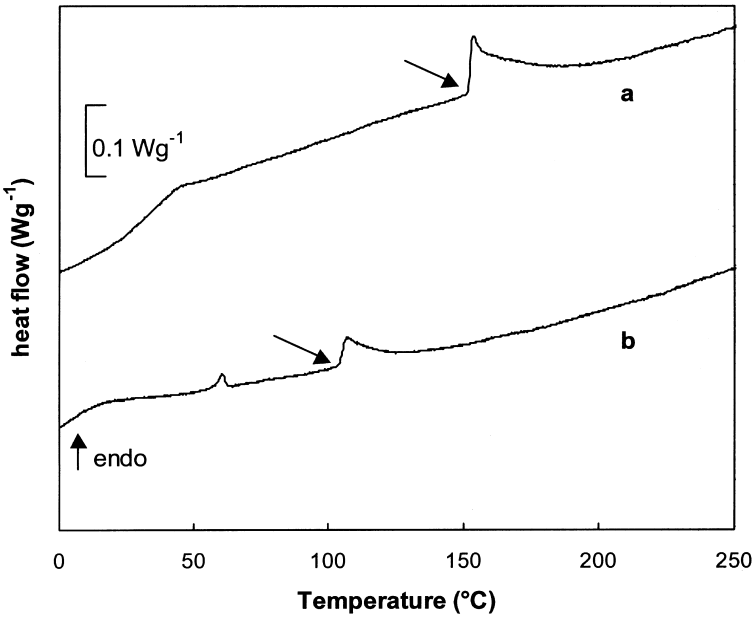

Fig. 2. Conventional DSC thermograms at a heating rate of 10°C min^{-1} of a 50/50 blend of: (a) PEO/Aramide; and (b) PEO/PES.

temperature. The quenching procedure is intended to avoid crystallization of PEO, which would interfere with the determination of T_g of the blend. Fig. 2 shows a single glass transition for the PEO/Aramide system, as an indication of an initially homogeneous blend. The difficulty of the quenching procedure is illustrated with the thermogram of the PEO/PES blend, still showing a very small melting peak of PEO around 60°C. For the same content of PEO in the homogeneous blends, PEO/PES is crystallizing faster than PEO/Aramide. Moreover, the higher the PEO content, the less efficient the quenching procedure to avoid crystallization in both homogeneous systems [25,26].

An endothermic signal is observed with an onset temperature at 152 and 103°C, respectively (indicated by arrow). They correspond to the cloud point temperatures measured by optical microscopy for both 50/50 blends (see Table 1).

The shape of the evolved heat flow signal depends strongly on the blend composition. It was reported in literature that the area of the endothermic phase separation signal in a conventional DSC experiment is related to the enthalpy of demixing, ΔH_{demix} [2]. ΔH_{demix} of a low molecular weight system was theoretically calculated from the enthalpy differences of the demixed phases, and a theoretical heat flow signal was obtained from the derivative of ΔH_{demix} with respect to temperature. This theoretical DSC signal

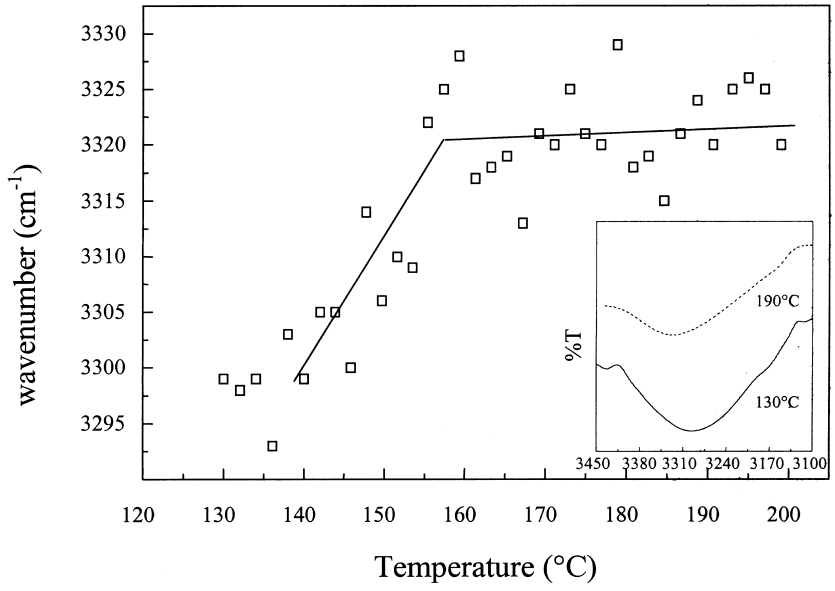

Fig. 3. Evolution of the FTIR wavenumber of the N–H stretching vibration of a 50/50 PEO/Aramide during heating at 1.5°C min^{-1}.

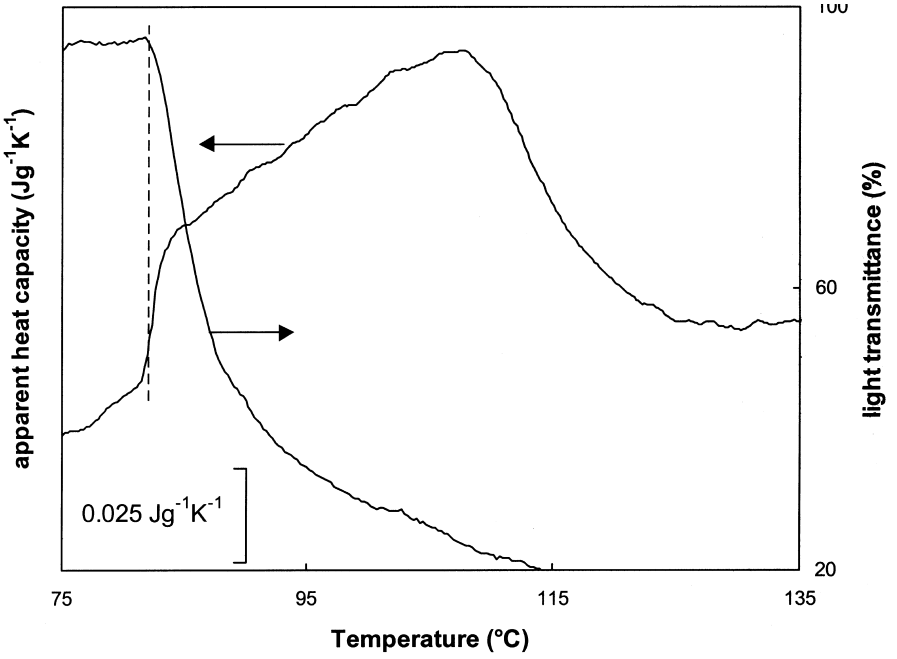

Fig. 4. MTDSC experiment (apparent heat capacity) and optical microscopy measurement (% light transmittance) of a 75/25 PEO/PES blend: underlying heating rate $\beta = 1°C\ min^{-1}$, modulation amplitude $A_T = 1°C$ and period $p = 60$ s (1°C/60 s).

showed an endothermic peak with a sharp low-temperature side and a slow decrease to the baseline at the high-temperature side, corresponding to a phase separation process during which the composition of the co-existing phases changes continuously as a function of increasing temperature [2]. Although the quality of these rather small endothermic signals is insufficient for a clear interpretation of the demixing enthalpy versus composition, it can be observed from Fig. 2 that ΔH_{demix} of the PEO/Aramide blend is at least twice that of the PEO/PES blend. This doubled value ($\Delta H_{demix} = 5.0 \pm 0.5\ J\ g^{-1}$ for a 50/50 PEO/Aramide blend) can be assigned to the presence of hydrogen bonds in the homogeneous PEO/Aramide blends, which contribute to a higher interaction energy and a higher demixing enthalpy [27–29].

The presence of hydrogen bonds and their importance in the phase separation process of PEO/Aramide blends is shown with FTIR analysis. The broad absorption band from 3400 to 3100 cm^{-1} of the N–H stretching vibration mode of the 50/50 PEO/Aramide blend shifts to higher wavenumber with increasing temperature (Fig. 3). As free N–H groups are absorbing at higher wavenumber than hydrogen bonded N–H groups, the observed shift is assigned to the fact that hydrogen bonds are disfavored at higher temperature. An increase of the wavenumber of the N–H absorption band is observed around the cloud point temperature of 150°C, indicating the important exchange of hydrogen bonds in this temperature domain.

3.1.3. MTDSC

In a next step, the onset of the liquid–liquid phase separation process was investigated by means of MTDSC. The PEO/PES blend, revealing the smaller endothermic conventional DSC signal at phase separation, was used for this purpose. For the 75/25 PEO/PES system, using conventional DSC, a heating rate of at least 10°C min^{-1} is needed for a reproducible calculation of the onset temperature of demixing and of the small value of the demixing enthalpy of the broad demixing endotherm ($\Delta H_{demix} < 2\ J\ g^{-1}$ smeared-out over more than 50°C).

Fig. 4 shows an overlay of the heat capacity signal of an MTDSC experiment and the light transmittance of an optical microscopy measurement of the 75/25 PEO/PES system, both at a low heating rate of 1°C min^{-1}. The onset of phase separation from optical microscopy corresponds very well to the onset of a small stepwise increase in the MTDSC heat capacity. This observation is also valid for the other blend compositions of PEO/PES and for PEO/Aramide blends (see Table 1). MTDSC reliably measures these small heat capacity changes as a function of temperature, omitting noise and baseline curvature [8–10]. Using conventional DSC, a heating rate of 1°C min^{-1} is too low to detect the onset temperature of demixing and to reproducibly calculate the small value of the demixing enthalpy. The ability to detect the onset of phase separation in polymer blends by means of the MTDSC heat capacity signal is therefore superior to the conventional DSC method, especially at low heating rates.

The question rises whether the stepwise increase (and also the further evolution) of the cyclic or (modulus of) complex heat capacity, C_p, calculated according to Eq. (1) and depicted in Fig. 4, depends solely on the thermodynamic heat capacity of the blend, or also on an 'excess' contribution caused by the enthalpic effects from the

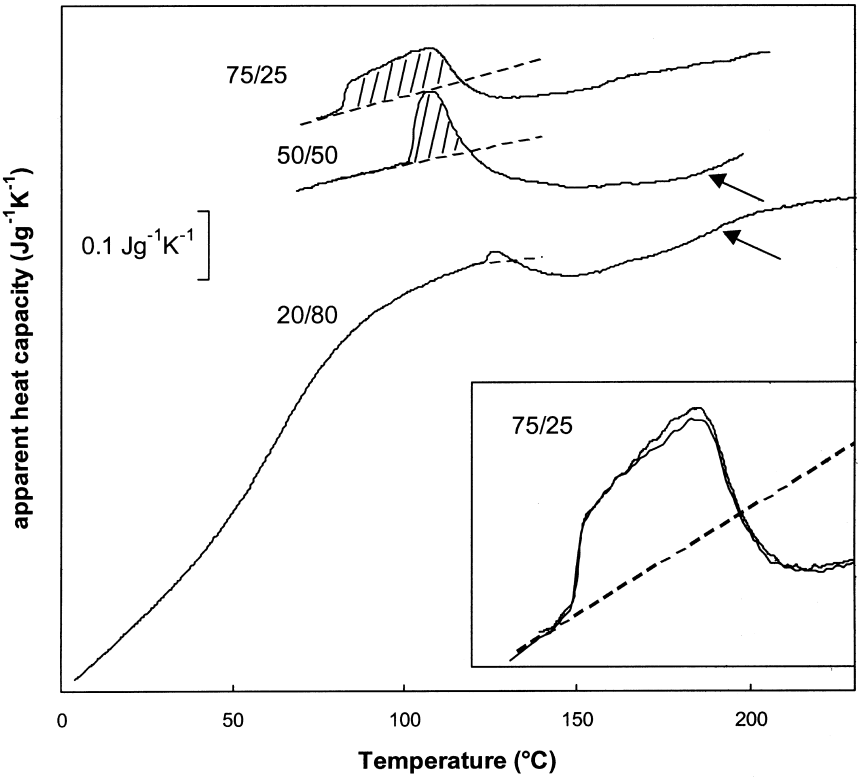

Fig. 5. Apparent heat capacity of PEO/PES blends (75/25, 50/50 and 20/80) at an underlying heating rate $\beta = 1°C\ min^{-1}$ and modulation of 1°C/60 s; the hatched areas show the enthalpic effect associated with the demixing process; two independent measurements for the 75/25 blend show the reproducibility (enlarged insert).

phase separation process (see further discussion). For this reason, the heat capacity signal of Fig. 4 is referred to as 'apparent' heat capacity in order to emphasize the difference with the pure thermodynamic heat capacity of the system.

3.2. Evolution of demixing with temperature and time as detected by MTDSC

After a comparison of the onset temperatures of phase separation by means of optical microscopy, conventional DSC and MTDSC, the discussion is extended to the evolution of the global phase separation process as detected by MTDSC. For this purpose the 'apparent' heat capacity signal beyond the onset of phase separation is considered.

3.2.1. Non-isothermal demixing

Fig. 5 shows that the composition of the PEO/PES blend has a marked effect, not only on the onset temperature of phase separation, but also on the apparent heat capacity evolution afterwards. The observed heat capacity changes are small (much less than $0.1\ J\ g^{-1}\ K^{-1}$ for most compositions) in comparison to the heat capacity change in the glass transition region of the homogeneous blends (see heat capacity change at T_g around 70°C for the 20/80 PEO/PES system). Despite these small changes in heat capacity, the reproducibility of the onset temperature of the sudden heat capacity increase and of the further evolution of the apparent heat capacity signal is very satisfactory (see insert of Fig. 5 for the 75/25 PEO/PES blend). It illustrates the power of MTDSC to detect these effects during the non-isothermal phase separation process.

The extrapolation of the heat capacity evolution before the onset of phase separation is depicted with a dashed line as a guide to the eye. Assuming a simple additivity rule as a first approximation, this temperature dependency can be predicted using reference values for PEO and PES from the ATHAS database [30]. For all three blend compositions shown in Fig. 5, the extrapolated heat capacity evolution enables to distinguish two temperature domains.

Firstly, at temperatures beyond the cloud point temperature, an 'excess' heat capacity contribution is observed due to the enthalpic effects associated with the demixing process. The enthalpy content of this excess contribution (shaded area in Fig. 5) is at least $1\ J\ g^{-1}$ for the 50/50 PEO/PES blend, comparable with values obtained with conventional DSC at $10°C\ min^{-1}$ ($\Delta H_{demix} < 2\ J\ g^{-1}$). It indicates that ΔH_{demix} is for the larger part retrieved in the apparent heat capacity (or 'reversing' heat flow signal). The 'non-reversing' heat flow (with noise and baseline curvature) and the (corrected) heat flow phase of the same MTDSC experiment are very small in magnitude. So, the information of the MTDSC *total* heat flow signal (coinciding with the conventional DSC thermogram at the same average heating rate [8]) is almost entirely retrieved in the

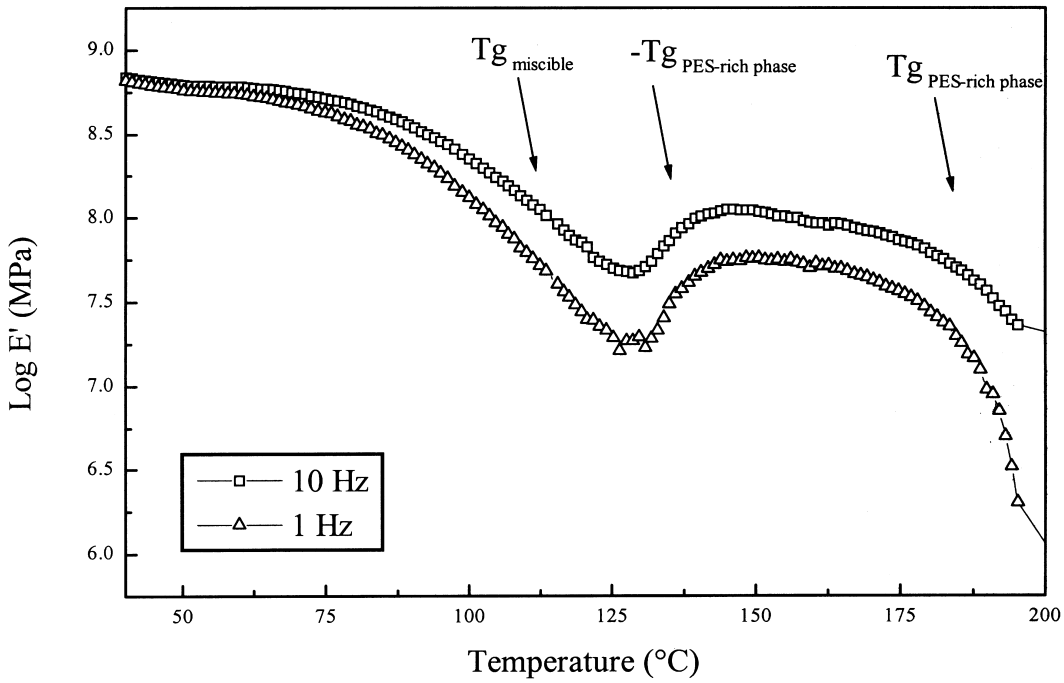

Fig. 6. Storage modulus E' (DMTA) of a 20/80 PEO/PES blend at 1 and 10 Hz during heating at 2°C min^{-1}.

MTDSC reversing heat flow signal. The partition between reversing and non-reversing contributions depends on the properties of the polymer blend system and on the modulation conditions. As an example, the non-reversing heat flow for the 50/50 PEO/Aramid system is ca. 30% of the total heat flow.

Secondly, at even higher temperatures (beyond ca. 125°C), a lower value of the heat capacity is noticed. This decrease in heat capacity is caused by a dominating effect of (partial) vitrification. During the liquid–liquid phase separation process, a PEO-rich and a PES-rich phase are created. If the amount of high-T_g component (PES) in the PES-rich phase becomes sufficiently high, (partial) vitrification of this phase might occur, resulting in a decrease of the thermodynamic heat capacity [16]. In addition, blends with higher amounts of PES (50/50 and 20/80) clearly show a devitrification effect (increase in heat capacity) at the highest temperatures, subsequent to the vitrification effect at intermediate temperatures (see arrows in Fig. 5).

The findings of vitrification and devitrification of the PES-rich phase, as detected in real-time by MTDSC, are clearly supported by a DMTA experiment of the 20/80 PEO/PES blend, as shown in Fig. 6. The storage modulus E' decreases around 100°C, the glass transition region of the miscible blend. Immediately after phase separation at 120°C, E' increases due to the vitrification of the PES-rich phase; from 190°C this phase devitrifies and the storage modulus decreases again (compare with Fig. 5).

It should be mentioned that the contribution to the thermodynamic heat capacity of (i) the interactions between the different components in the homogeneous blend and (ii) the large interfacial area of a two-phase system created upon demixing is still uncertain [31]. However, these effects should be considered for a proper description of the evolution of the thermodynamic heat capacity (‘reference’ or ‘baseline’ heat capacity) of the blend system. The temperature dependency of this baseline heat capacity, in relation to excess contributions, vitrification and devitrification, is important for a correct calculation of ΔH_{demix}.

The interpretation of Fig. 5 illustrates that the theoretical heat flow curve of a conventional DSC thermogram, as predicted in Ref. [2], should be treated with caution if applied to polymer blends. Other aspects like time-dependent behavior with diffusion restrictions and vitrification can play an important role in the phase separation process.

3.2.2. Isothermal demixing

Two different processes can be associated with the development of a phase-separated morphology: a ‘thermodynamically driven’ structure formation, and a kinetically controlled compositional evolution of the co-existing phases [32]. The first process corresponds to the cloud point measured non-isothermally in Fig. 5, while the second process is important for the excess heat capacity contribution and eventual partial (de)vitrification of a PES-rich phase at higher temperatures.

To gain insight into the time dependency or the kinetics of the demixing process, isothermal demixing experiments are of interest. Controlled heating to the isothermal temperature is preferred in this study: (i) to check the reproducibility of the heat capacity evolution of the non-isothermal path up to the isothermal temperature; and (ii) to enable the comparison of isothermal and non-isothermal demixing curves. Fig. 7 shows the evolution of the apparent heat capacity for two

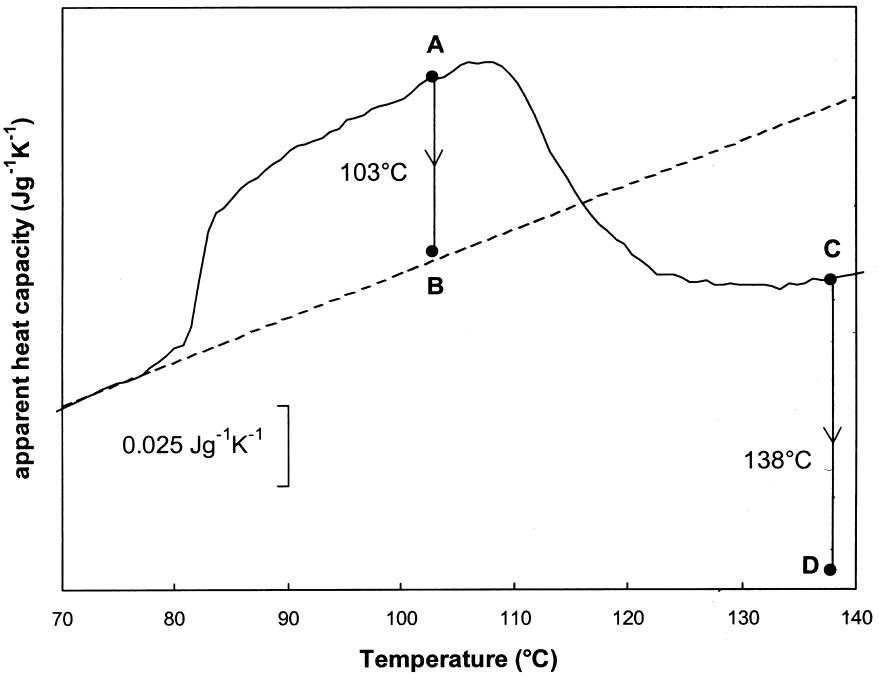

Fig. 7. Apparent heat capacity of a 75/25 PEO/PES blend at an underlying heating rate $\beta = 1°C\ min^{-1}$ and modulation of 1°C/60 s; the subsequent decrease in apparent heat capacity during quasi-isothermal demixing at 103°C (arrow from A to B) or 138°C (arrow from C to D) is shown too (see also Fig. 8).

combined paths of controlled heating at $1°C\ min^{-1}$ followed by isothermal demixing at 103 or 138°C (isothermal paths indicated by vertical arrows from A to B and C to D, respectively). These temperatures were chosen to study isothermal demixing without and with interference of vitrification, respectively. The apparent heat capacity of the (quasi-) isothermal demixing steps at 103 and 138°C are shown as a function of demixing time in Fig. 8.

Demixing at 103°C results in a decrease of the apparent heat capacity, which can be attributed to a time-dependent evolution of the composition of the co-existing phases. The limiting value at the end of the process

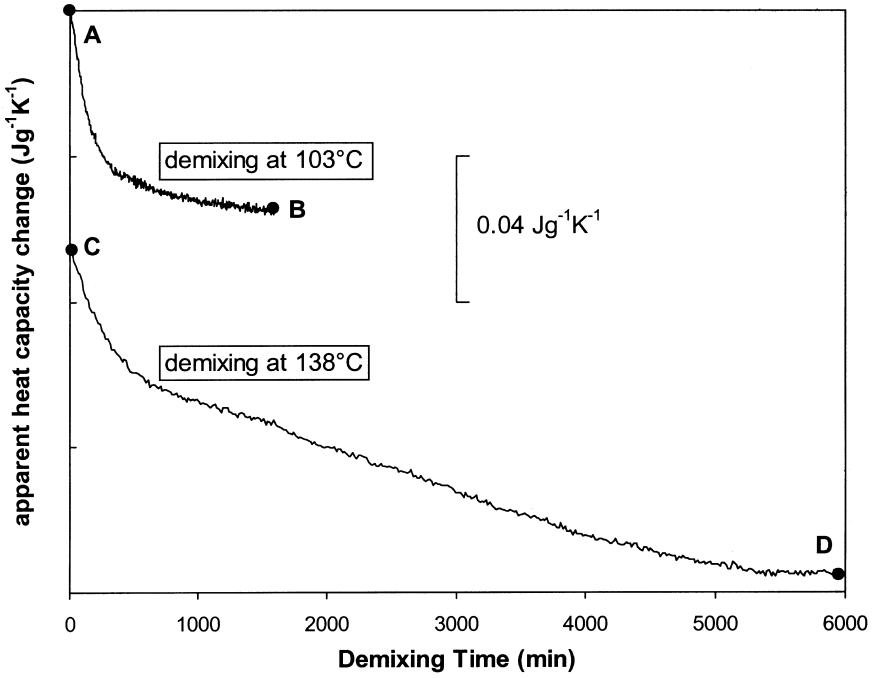

Fig. 8. Quasi-isothermal apparent heat capacity as a function of time of demixing at 103 and 138°C of a 75/25 PEO/PES blend; modulation of 1°C/60 s.

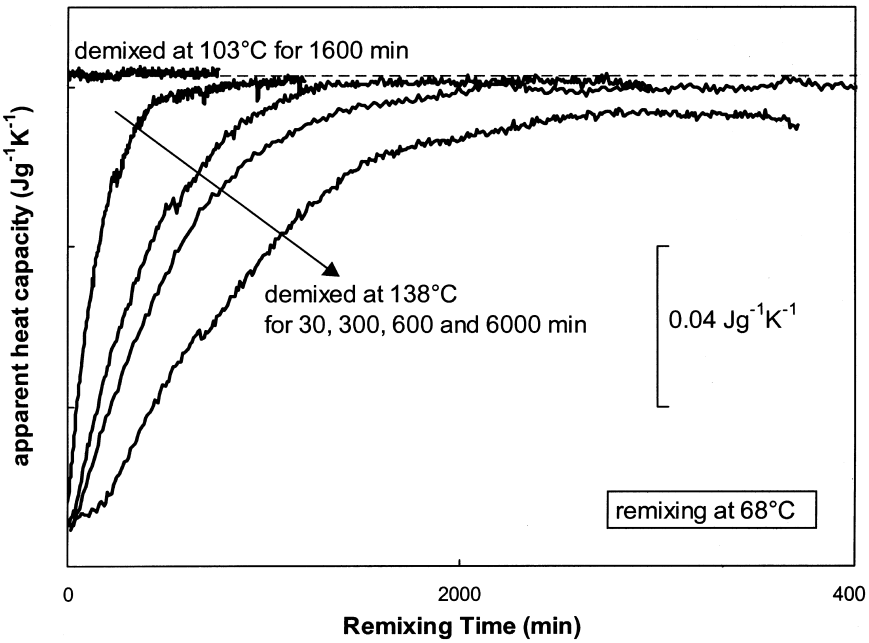

Fig. 9. Quasi-isothermal apparent heat capacity as a function of time of remixing at 68°C of a 75/25 PEO/PES blend after: (i) demixing at 103°C for 1600 min; and (ii) demixing at 138°C for 30, 300, 600 and 6000 min; modulation of 1°C/60 s.

(point B in Fig. 7 and Fig. 8) is in agreement with the predicted thermodynamic value for the blend at 103°C, according to a simple additivity rule applied on literature values for the heat capacities of PEO and PES (compare with dashed line in Fig. 7 [30]). For the PEO/PES system, no obvious deviation baseline heat capacity seems to occur during phase separation, so that specific interactions present in homogeneous conditions (e.g. at 68°C) or developed at the interface in heterogeneous conditions (e.g. at 103°C) are probably not important or at least seem to cancel each other. Note that demixing after an immediate temperature jump to 103°C shows almost the same behavior as the controlled-rate experiment. This indicates that the initial formation of the phase-separated structure occurs in a time scale shorter than the stabilization time of the instrument after an immediate jump.

The decrease of the heat capacity at 138°C is even larger and is primarily the result of a time-dependent (partial) vitrification of the PES-rich phase. This vitrification process at 138°C is in agreement with the observations during non-isothermal demixing (see Fig. 5). The observed decrease in heat capacity by vitrification is obviously more pronounced in isothermal demixing conditions (compare positions C and D in Fig. 7 and Fig. 8).

The kinetics of the demixing process, influenced by diffusion across the interface or interphase of the co-existing phases and by vitrification of the high-T_g phase, are important for the final properties of the binary blend. During heating at 1°C min^{-1}, the composition of the co-existing phases changes continuously, but the equilibrium compositions are never attained at intermediate temperatures. After long isothermal demixing times, however, the PEO/PES system tends to the final equilibrium compositions of the co-existing phases.

3.3. Kinetics of demixing and remixing

The kinetics of demixing and remixing and the interrelations of these processes was investigated by the following temperature/time cycle: (i) heating of the miscible 75/25 PEO/PES blend from 68°C (a temperature below the cloud point curve but above the melting temperature of PEO, within the miscible temperature/composition region of the phase diagram, see Fig. 1b) to a temperature above the cloud point curve (e.g. 103 and 138°C), and after a certain isothermal demixing time, (ii) rapid cooling (temperature jump) of the demixed system again to 68°C, and after remixing for a certain time, (iii) final reheating at 1°C min^{-1} to a temperature above the cloud point curve.

3.3.1. Influence of temperature and time of demixing on kinetics of isothermal remixing

The experimental conditions of Figs. 7 and 8 were taken as starting point for step (i). Appropriate demixing times were determined according to the quasi-isothermal MTDSC experiments at 103 and 138°C of Fig. 8. Isothermal remixing at 68°C of these phase-separated 75/25 PEO/PES samples (step (ii)) is depicted in Fig. 9.

For demixing at 103°C, no influence of the demixing time is noticed. Even after demixing for as long as 1600 min, the measured heat capacity at 68°C is immediately at the reference value of the thermodynamically stable remixed state (indicated by horizontal dashed line in Fig. 9). It proves that the remixed state is already attained during the temperature

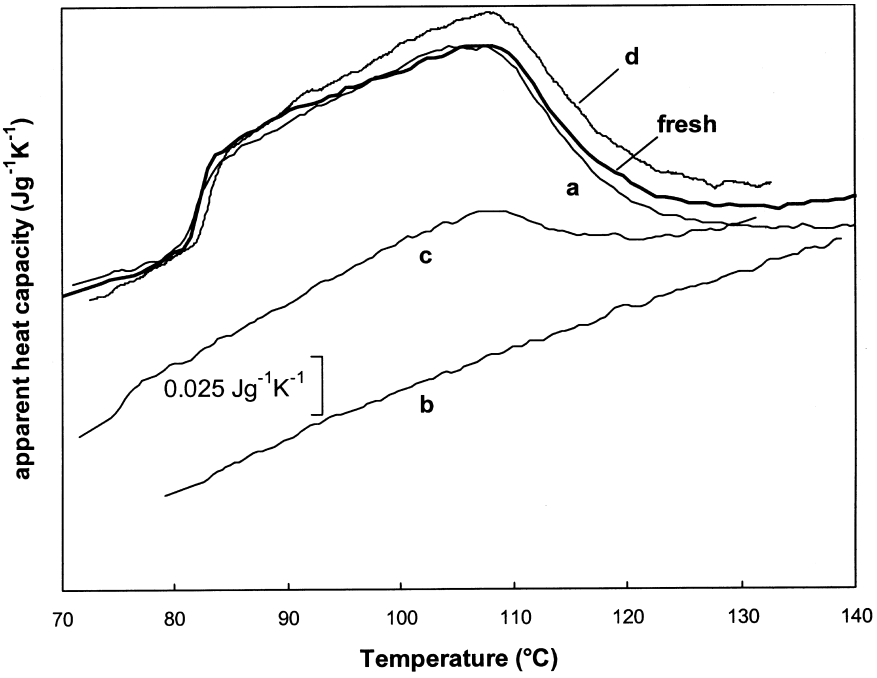

Fig. 10. Apparent heat capacity of a 75/25 PEO/PES blend at an underlying heating rate $\beta = 1°C\ min^{-1}$ and modulation of 1°C/60 s after: (i) demixing at 103°C for 1600 min (see Fig. 8) and remixing shortly at (a) 68°C; and (ii) demixing at 138°C for 6000 min (see Fig. 8) and remixing at 68°C for (b) 0; (c) 600; and (d) 3000 min. The apparent heat capacity curve of Fig. 7 is given for comparison ('fresh').

jump to 68°C. This finding is supported by a light scattering experiment following the same temperature program, where, immediately after cooling down to 68°C, the transmitted light intensity of the homogeneous sample was observed. Vitrification is avoided during demixing at 103°C and even after cooling to 68°C, since the glass transition of the PES-rich phase is sufficiently low in these conditions (see predicted glass transition curve of Fig. 1 and also results of Fig. 10).

During demixing at 138°C, however, a (partial) vitrification of the PES-rich phase is interfering. This vitrification effect is further intensified by lowering the temperature. After phase separation at 138°C and the temperature jump to 68°C, a gradual increase of the apparent heat capacity is observed during remixing at 68°C due to the devitrification of the frozen out PES-rich phase. Only after a long remixing time (see time scale of Fig. 9), the thermodynamically stable remixed state is approached. In contrast with the system demixed at 103°C, the time of demixing at 138°C is important. Longer demixing times at 138°C result in a slower remixing at 68°C caused by a more diffusion-restricted devitrification process.

The results of Fig. 9 are in agreement with the phase diagram and the predicted glass transition curve for the PEO/PES blend (see Fig. 1b). An interesting comparison can be made with the PEO/Aramide system (Fig. 1a). In the latter system, vitrification is not expected to occur during demixing, due to the higher LCST curve with respect to the glass transition curve. This prediction was confirmed by demixing a 50/50 PEO/Aramide blend at 185°C: the remixing step at 135°C occurs immediately or at least within the time scale of the temperature jump to 135°C, without interference of a decelerating devitrification process.

3.3.2. Influence of time of remixing on non-isothermal demixing

Results for non-isothermal demixing after remixing at 68°C (step (iii) of the demixing/remixing temperature cycle) are shown in Fig. 10. These are an immediate consequence of the results of Fig. 9.

It shows that, after demixing at 103°C for 1600 min (see Fig. 8), remixing shortly at 68°C (see Fig. 9) is sufficient to obtain a material with the same non-isothermal phase separation behavior as a freshly prepared 75/25 PEO/PES sample. Not only the cloud point temperature of the remixed blend, but also the evolution beyond this stage is identical (Fig. 10, compare curve a with 'fresh').

A sample demixed at 138°C for 6000 min (see Fig. 8), on the contrary, shows no remixing after a short time at 68°C (see Fig. 9). Therefore, if the sample is heated again, no cloud point temperature is detected and the sample is gradually devitrifying with increasing temperature (Fig. 10, curve b). After remixing 600 min at 68°C, the non-isothermal phase separation of a partially remixed blend is seen (Fig. 10, curve c). A remixing time of at least 3000 min at 68°C is necessary to attain approximately the same non-isothermal phase separation behavior of the fresh sample (Fig. 10, compare curve d with 'fresh').

From the combined information of Figs. 7–10, it is obvious that the kinetics of demixing/remixing of the

PEO/PES blend depends on the temperature/time combinations of the steps involved. The kinetics of the diffusion-controlled processes at the interface between the co-existing phases and vitrification/devitrification effects of the PES-rich phase play an important role.

4. Conclusions

MTDSC proves to be useful for the determination of the cloud point temperature associated with phase separation in polymer blends showing LCST behavior. The demixing process can be followed in the apparent heat capacity which is influenced by two major effects: (i) the enthalpy of demixing primarily at temperatures beyond the cloud point (e.g. 103°C), which can be associated with the evolution in the composition of the co-existing phases; and (ii) vitrification effects at higher temperatures (e.g. 138°C), resulting from the formation of a high-T_g co-existing phase.

The ability of MTDSC to measure the apparent heat capacity in quasi-isothermal conditions has been exploited to follow demixing and remixing, and the interrelation between both processes. If vitrification occurs during demixing, a slow devitrification of the high-T_g phase is necessary to attain the thermodynamically stable remixed state.

The quasi-isothermal MTDSC measuring mode enables one to gain insight in the kinetics of the remixing/demixing processes and can contribute to a better understanding of the real-time morphology development of partially miscible polymer blends.

Acknowledgements

The work of S.S. was supported by grants of the Flemish Institute for the Promotion of Scientific-Technological Research in Industry (I.W.T.). This research project was financially supported by the Research Council K.U. Leuven and the Fund for Scientific Research Flanders (FWO-Vlaanderen).

References

[1] Vanneste M, Groeninckx G. Polymer 1994;35:1051.
[2] Arnauts J, De Cooman R, Vandeweerdt P, Koningsveld R, Berghmans H. Thermochim Acta 1994;238:1.
[3] Shen S, Torkelson JM. Macromolecules 1992;25:721.
[4] Natansohn A. J Polym Sci: Polym Lett Ed 1985;23:305.
[5] Ebert M, Garbella RW, Wendorff JH. Makromol Chem Rapid Commun 1986;7:65.
[6] ten Brinke G, Oudhuis L, Ellis T. Thermochim Acta 1994;238:75.
[7] Dompas D, Isogawa M, Hasegawa T, Kadokura M, Groeninckx G. Polymer 1997;38:421.
[8] Reading M. Trends Polym Sci 1993;8:248.
[9] Reading M, Elliot D, Hill VL. J Thermal Anal 1993;40:949.
[10] Gill PS, Sauerbrunn SR, Reading M. J Thermal Anal 1993;40:931.
[11] Reading M, Luget A, Wilson R. Thermochim Acta 1994;238:295.
[12] Wunderlich B, Jin Y, Boller A. Thermochim Acta 1994;238:277.
[13] Van Assche G, Van Hemelrijck A, Rahier H, Van Mele B. Thermochim Acta 1995;121:268.
[14] Van Assche G, Van Hemelrijck A, Rahier H, Van Mele B. Thermochim Acta 1996;209:286.
[15] Van Assche G, Van Hemelrijck A, Rahier H, Van Mele B. Thermochim Acta 1997;304/305:317.
[16] Swier S, Van Assche G, Van Hemelrijck A, Rahier H, Verdonck E, Van Mele B. J Thermal Anal 1998;54:585.
[17] Swier S, Van Mele B. Thermochim Acta 1999;330:175.
[18] Inoue T. Progr Polym Sci 1995;20:119.
[19] VenderBosch R, Meijer HEH, Lemstra P. J Polym 1995;36:2903.
[20] Chen W, Kobayashi S, Inoue T, Ohnaga T, Ougizawa T. Polymer 1994;35:4015.
[21] Nakata S, Kakimoto M, Imai Y. Polymer 1992;33:3873.
[22] Gaur U, Wunderlich B. J Phys Chem Ref Data 1982;11:313.
[23] Walsh D, Singh V. Makromol Chem 1984;185:1979.
[24] Guo W, Higgins J. Polymer 1990;31:699.
[25] Dreezen G, Fang Z, Groeninckx G. Polymer 1999;40:5907.
[26] Dreezen G, Koch MHJ, Reynaers H, Groeninckx G. Polymer 1999;40:6451.
[27] Etxeberria A, Guezala S, Iruin JJ, de la Campa JG, de Abajo J. Polymer 1998;39:1035.
[28] Bhagwagar D, Painter P, Coleman M, Krizan T. J Polym Sci Polym Phys 1991;29:1547.
[29] Hu J, Painter P, Coleman M, Krizan T. J Polym Sci Polym Phys 1990;28:149.
[30] Gaur U, Wunderlich B. J. Phys. Chem. Ref. Data 1982;11:313 (ATHAS database on the World Wide Web: web.utk.edu/~athas/databank/intro.html).
[31] Song M, Hourston DJ, Pollock HM, Hammiche A. Polymer 1999;40:4763.
[32] Dreezen G, Ivanov DA, Nysten B, Groeninckx G. Polymer 2000;41:1395.